Bioinspired Heterobimetallic Photocatalyst (Ru II chrom –Fe III cat) for Visible-Light-Driven C–H Oxidation of Organic Substrates via Dioxygen Activation

Siddhant Singh, Divyanshu Nautiyal, Franck Thetiot, Nicolas Le Poul, Tapas Goswami, Arun Kumar, Sushil Kumar

A Bio-Inspired Heterobimetallic Photocatalyst (Ru^{II}_{chrom}–Fe^{III}_{cat}) for Visible-Light-Driven C-H Oxidation of Organic Substrates by Activating Dioxygen

Siddhant Singh[†], Divyanshu Nautiyal[†], Franck Thetiot[#], Nicolas Le Poul[#], Tapas Goswami[‡],Arun Kumar[†], Sushil Kumar[‡]*

[‡] Department of Chemistry, University of Petroleum and Energy Studies, Bidholi, Dehradun-248007, Uttarakhand, India. Email:*sushilvashisth@gmail.com*

[†] Department of Chemistry, School of Physical Sciences, Doon University, Dehradun-248001, Uttarakhand, India.

CEMCA CNRS UMR 6521 Université de Bretagne Occidentale 6 avenue Le Gorgeu, CS 93837, Brest 29238, France.

ABSTRACT: We report a bio-inspired heterobimetallic photocatalyst**Ru^{II}_{chrom}–Fe^{III}_{cat}** and its relevant applications towards visible-light-driven C–H bond oxidation of a series of hydrocarbons using O_2 as oxygen atom source. The Ru(II) centre absorbs visible light near 460 nm and triggers a cascade of electrons to Fe(III) to afford a catalytically active high-valent Fe(IV)=O species. The *in-situ* formed Fe(IV)=O has been employed for several high-impact oxidation reactionsin the presence of triethanolamine (TEOA) as the sacrificial electron donor.

Nature uses many iron (Fe) containing enzymes to insert oxygen atom into organic substrates by activating dioxygen (O_2) molecule.[1–7]Such oxygenase enzymes (heme or non-heme) promote reductive O_2 activation to generate a high-valent iron-oxo (Fe(IV)=O) species which acts as an active oxidant.[8–11] Despite their impressive efficacy in numerous organisms, the high potential of such enzymes in industries and laboratories is still hampered due to the limited stability and requirement of expensive reductant cofactor NAD(P)H.[12] Consequently, mimicking the structure and function of these enzymes to develop syntheticmodels has become a mainstay for modern-day research. After a breakthrough report on crystal structure analysis of Fe(IV)=O species by Nam, Que, and co-workers,[13] several bio-inspired Fe-based complexes have been developed.[14–31] However, most of them require a strong oxidizing agent e.g. H_2O_2, *t*BuOOH or PhIO to attain Fe(IV)=O formation.[14,15] Sometimes, these harsh oxidizing agents show poor selectivity to the catalytic product and lead to uncontrolled oxidation reactions.

Recent efforts in this field have thus sought to combine such iron catalysts with a visible-light sensitive chromophore to photogenerate Fe(IV)=O, in the presence of either H_2O or O_2 as oxygen atom source.[32–35] Inspired by pioneered works of Gray's group[36–38] on chromophore-CytP450 systems, many researchers demonstrated the possible photogeneration of iron-oxo using a mixture of non-heme iron catalyst and Ru(II)-chromophore in the presence of water.[39–43] Nevertheless, in majority of the cases reported so far, the photogeneration of Fe(IV)=O has been carried out using bimolecular chromophore/catalyst systems.[38–42,44–48] Unlike bimolecular systems, covalent linking of a chromophore with Fe-based catalytic fragment to form supramolecular photocatalysts must facilitate a successful and aligned e^- transfer with higher efficiency.To the best of our knowledge, there is only single report by Leibl, Aukauloo, Banse and co-workers[43] where non-heme Fe(IV)=O is photogenerated by a covalently bound Ru(II)–Fe(II) system even so with H_2O.

An alternative approach to generate iron-oxo would be a photoinduced reductive activation of O_2.[37,38] Though O_2 is an abundant and greenest oxidant, the photocatalytic aerobic oxidation reactions using non-heme Fe-based catalysts are rare.[44,45] Two parameters are essential to attain an efficient reductive O_2 activation at the catalytic site in such systems: i) a short distance between the chromophore and catalytic fragments and ii) relatively lower redox potential of the chromophore as compared to the catalytic unit. Covalent linking of $Ru(bpy)_3^{2+}$ based chromophore to Fe-TPA (TPA = tris(pyridin-2-ylmethyl)amine) based catalyst may act as an ideal photosystem as the excited $Ru(bpy)_3^{2+}$ has relatively lower oxidation potential.[43,49]

We report a unique example of heterobimetallic complex $[(bpy)_2Ru(imptp)Fe(Cl)]^{3+}$ (bpy = 2,2'-bipyridine; Himptp = *N*-((6-(*1H*-imidazo[4,5-*f*][1,10]phenanthrolin-2-yl)pyridin-2-yl)methyl)(pyridin-2-yl)-*N*-(pyridin-2-ylmethyl)methanamine), abbreviated here as **Ru^{II}_{chrom}–Fe^{III}_{cat}**. This complexconsists of a Ru^{II}-bpybased chromophorecovalently bound with a Fe(TPA)-catalyst *via* imidazole linker (Scheme 1a). Complex **Ru^{II}_{chrom}–Fe^{III}_{cat}** has been employed as photocatalyst for pertinent visible-light-driven C–H oxidation of different hydrocarbons. Exposure of photogenerated **Ru^{II}–Fe^{II}** to

O_2 leads to the formation of **Ru^{II}–Fe^{IV}–oxo** intermediate as a key oxidant for substrate oxidation (Scheme 1b).

Scheme 1. (a) Chemical drawings of Ru^{II}_{chrom} and Ru^{II}_{chrom}–Fe^{III}_{cat}. (b) Proposed electron flow for substrate oxidation by Ru^{II}_{chrom}–Fe^{III}_{cat}.

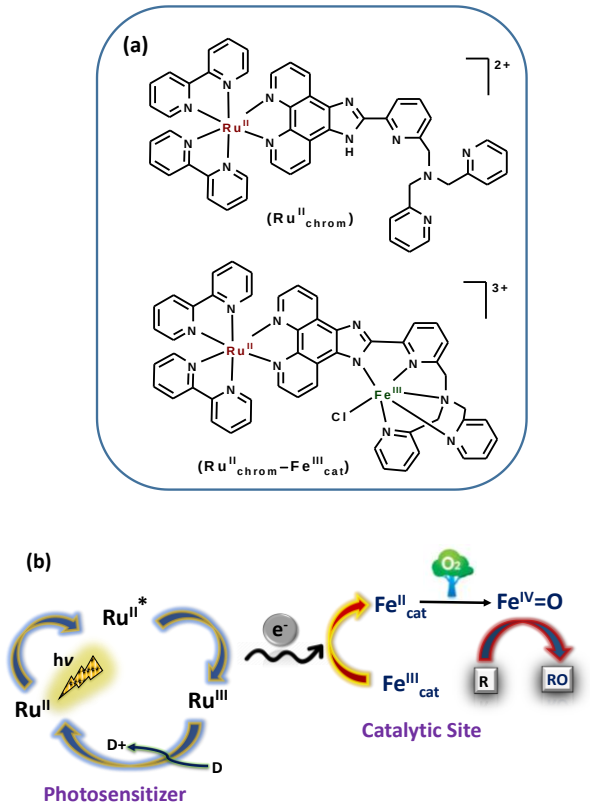

To synthesize **Ru^{II}_{chrom}–Fe^{III}_{cat}**, first, a monometallic complex $[(bpy)_2Ru(Himptp)]^{2+}$,abbreviated as **Ru^{II}_{chrom}**, was prepared by refluxing *cis*-$Ru(bpy)_2Cl_2$ with ligand Himptp (Scheme S1).Complex $[(bpy)_2Ru(Himptp)]^{2+}$ was then treated with anhydrous $FeCl_3$ to obtain **Ru^{II}_{chrom}–Fe^{III}_{cat}**.^{1}H NMR spectra of Himptp and **Ru^{II}_{chrom}**clearly revealed all the expected resonances (Figures S3–S4). A singlet at 14.01 ppm was assigned to -NH- group of imidazole ring in free ligand.[50] Two singlets near 3.89 ppm and 4.05 ppm wereassignedto $–CH_2$-pyridine moieties of TPA unit. Furthermore, the ESI-MS study for **Ru^{II}_{chrom}** measured an exact mass of 1213.1915 corresponding to protonated molecular ion $[M + H]^+$ coinciding well with the theoretical value of 1213.1904 (Figure S7).

The structure of **Ru^{II}_{chrom}–Fe^{III}_{cat}** was established by single-crystal XRD analysis (Figure S1). BothRu(II) and Fe(III) adopt a pseudo-octahedral geometry. All the bond parameters concerning the metal cores in **Ru^{II}_{chrom}–Fe^{III}_{cat}** (Tables S1–S2) are consistent with the data reported earlier for Fe[41,49] and Ru[50,51] analogues.Notably, the relatively short distance between Ru and Fe (8.328 Å)may promote a facile electron tunneling between the redox partners.[52,53]

UV–visible spectra of **Ru^{II}_{chrom}** and **Ru^{II}_{chrom}–Fe^{III}_{cat}** in deaerated acetonitrile solutions exhibit a broad absorption band near 460 nm (MLCT, $d\pi_{Ru}$–π^*_{bpy})(ε/$M^{-1}cm^{-1}$ = 15,625 for **Ru^{II}_{chrom}** and 14,000for **Ru^{II}_{chrom}–Fe^{III}_{cat}**) (Figure 1a).[54–56] In **Ru^{II}_{chrom}–Fe^{III}_{cat}**, the band near 360 nm has been assigned to Fe-centered transition.This band coincides well with the absorption maxima observed in the parental $Fe(TPA)Cl_2$ and its derivatives.[43,49]Excitation with 468 nm light resulted in bright-orange luminescence of **Ru^{II}_{chrom}** with an emission maxima centered at 614 nmin deaerated acetonitrile. Noteworthy, the luminescence intensity is significantly quenched (upto 70%) in **Ru^{II}_{chrom}–Fe^{III}_{cat}** (Figure 1b) which may be typically attributed to photoinduced e^-or energy transfer process from excited chromophore to catalytic Fe center.[54–56]

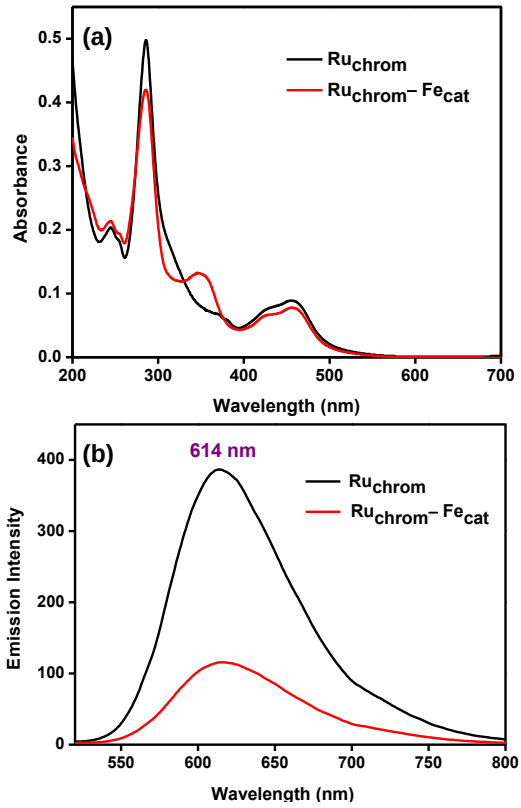

Figure 1. (a) UV–visible and (b) emission spectra of **Ru^{II}_{chrom}** (~5.5 x 10^{-6} M)and **Ru^{II}_{chrom}–Fe^{III}_{cat}** (~5.5 x 10^{-6} M)in deaerated acetonitrile solution.

To assess the electronic communication between two components in photocatalyst, the redox behavior of **Ru^{II}_{chrom}** and **Ru^{II}_{chrom}–Fe^{III}_{cat}** was investigated in degassed acetonitrile under inert atmosphere (Figure S10, Table S3). **Ru^{II}_{chrom}** displayed a reversible system upon

oxidation at $E_{1/2}$ = 1.27 V *vs.* SCE ($\Delta E_p = E_{pa} - E_{pc}$ = 71 mV), a value close to that of Ru-bpy derivatives ($E_{1/2}$ = 1.28 V *vs.* SCE).[55–57] A supplementary irreversible wave detected at 1.17 V can be assigned to the irreversible oxidation of free tertiary amine by direct comparison with $\mathbf{Ru^{II}_{chrom}–Fe^{III}_{cat}}$ (*vide infra*). Two reversible waves at –1.40 (ΔE_p = 48 mV) and –1.61 (ΔE_p = 86 mV) are attributed to the successive reductions of bpy ligands.[51,55–57]In case of $\mathbf{Ru^{II}_{chrom}–Fe^{III}_{cat}}$, the reversible oxidation of Ru^{II} occurred at $E_{1/2}$ = 1.26 V *vs.* SCE (Figure S10), similar to $\mathbf{Ru^{II}_{chrom}}$.An additional reversible system was detected at $E_{1/2}$ = 0.56 V (ΔE_p = 59 mV), assigned to the $Fe^{III/II}$ redox couple in agreement with reported data for analogous pyridyl-coordinated Fe-Cl complexes.[43,49] On the basis of experimental data which showed that the oxidation of the Ru(II) center in $\mathbf{Ru^{II}_{chrom}–Fe^{III}_{cat}}$ occurs at a very close potential value to that of $Ru(bpy)_3^{2+}$, we have approximated the standard potential of the $Ru^{III/II*}$ couple (in its excited state) for $\mathbf{Ru^{II}_{chrom}–Fe^{III}_{cat}}$ to that of $Ru(bpy)_3^{2+}$, i.e. E_o = –0.72 V *vs.* SCE.[55,57] Consequently, the transfer of one electron from Ru^{II*} to Fe^{III} may be thermodynamically favored, leading to the generation of new Ru(III)–Fe(II) species. This assumption is in agreement with our spectroscopic studies which demonstrate luminescence quenching when iron is present (Figure 1b), thus evidencing a favored photoinduced e^- transfer.

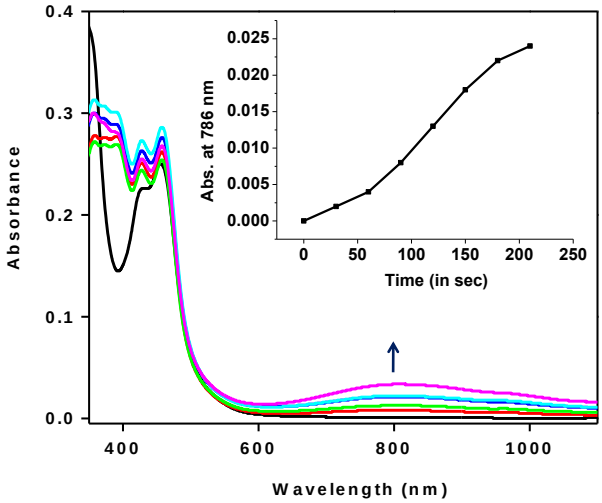

Figure 2. UV–visible spectral changes upon illuminating CH_3CN solution (LED; 468 nm) of $\mathbf{Ru^{II}_{chrom}–Fe^{III}_{cat}}$ in presence of TEOA and O_2. Inset: Kinetic traces at 786 nm.

The next step has thus consisted of reacting the insitu generated Fe(II) species with O_2. For that purpose, a sacrificial e^- donor TEOA was used to promote the return of Ru(III) ion to ground state.[38,44,57] A solution of $\mathbf{Ru^{II}_{chrom}–Fe^{III}_{cat}}$ with TEOA was thus subjected to a cycle of deoxygenation, light illumination at 468 nm, and O_2 exposure. The absorption spectra after each cycle indicated that exposure to O_2, after irradiation, exhibited a broad band at λ_{max} = 786 nm (Figure 2). Noteworthy, this band was not detected for $\mathbf{Ru^{II}_{chrom}}$ under the same reaction conditions, nor in the absence of any of the photocatalytic components (catalyst, TEOA, light or O_2). Thus, it clearly shows that the reaction implies Fe(II) center, which led us to assign it to the high-valent Fe(IV)=O species, consistent with the previous reports.[39–43,49]

Encouraged with the light-induced e^-transfer and subsequent Fe(IV)=O formation, $\mathbf{Ru^{II}_{chrom}–Fe^{III}_{cat}}$was investigated for visible-light-driven oxidation reactions under O2 atmosphere. The preliminary tests were performed with cyclohexane as substrate. In duration of 6 hours, $\mathbf{Ru^{II}_{chrom}–Fe^{III}_{cat}}$provided a TON of 66.5 with remarkable alcohol selectivity of 9.8 (Table 1; entry 1). A relatively low catalytic conversion (TON = 16.7) was observed without TEOA, probably due to theintervention of a competitive oxidation process (Table 1; entry 2) (*vide supra*).

Table 1. Optimization of photocatalytic oxidation of cyclohexane.

Entry	Cat. / Chrom.	Sacrif. donor	Atmos.	TON[a]	A/K
1.	$\mathbf{Ru^{II}_{chrom}–Fe^{III}_{cat}}$	TEOA	O_2	66.5	9.8
2.	$\mathbf{Ru^{II}_{chrom}–Fe^{III}_{cat}}$	-	O_2	16.7	6.5
3.	$\mathbf{Ru^{II}_{chrom}–Fe^{III}_{cat}}$	TEOA	N_2	traces	-
4.[b]	$\mathbf{Ru^{II}_{chrom}–Fe^{III}_{cat}}$	TEOA	O_2	73.6	12.6
5.[b]	$\mathbf{Ru^{II}_{chrom}–Fe^{III}_{cat}}$	TEOA	O_2	74.8	12.5
6.	- / $\mathbf{Ru^{II}_{chrom}}$	TEOA	O_2	11.0	2.6
7.[b, c]	$\mathbf{Fe(TPA)Cl_2}$ / $\mathbf{[Ru(bpy)_3]^{2+}}$	TEOA	O_2	22.9	7.6

Reaction conditions: Cyclohexane (0.5 mmol), Catalyst (0.93 mol %), TEOA (250 mol %), in CH_3CN: CH_2Cl_2: H_2O (3:1:1), LED irradiation (468 nm), O_2 bubbling. yields were calculated by GC-FID, duration: 6 h except entry 5 (8 h), [b]one drop CH_3COOH, [c]$Fe(TPA)Cl_2$ (1 mol%), $[Ru(bpy)_3]^{2+}$ (4 mol%), TEOA (15 mol %) A/K: alcohol/ketone ratio. Abbreviations: Cat. = Catalyst; Chrom. = Chromophore; Sacrif.= Sacrificial; Atmos. = Atmosphere.

Catalytic reactions under inert atmosphere provided the traces of oxidation products validating the role of O_2 as oxygen source (Table 1; entry 3). A slight conversion was also noticed (TON = 11.0) with $\mathbf{Ru^{II}_{chrom}}$, with a low selectivity towards cyclohexanol (Table 1; entry 6). This oxidation may proceed *via* $^1O_2$ formation by excited Ru^{II*}(Scheme 2).[58] In order to compare the catalytic efficacy of a covalently linked chromophore/catalyst system with that of a bimolecular system, we have employed a mixture of $Ru(bpy)_3^{2+}$ and $Fe(TPA)Cl_2$ (individually synthesized)[49] as catalyst (Table 1; Entry 7). Interestingly, $\mathbf{Ru^{II}_{chrom}–Fe^{III}_{cat}}$proved to be more efficient as the TON was increased upto 3.0-fold as compare to

bimolecular Ru_{chrom}/Fe_{cat} combination. Moreover, ca. 4.0-fold higher amount of chromophore was used to achieve this result in bimolecular system. The use of covalently linked assembly not only provides the greater efficiency, but also reduces the amount of expensive chromophores in the catalysis process. The substrate scope of $\mathbf{Ru^{II}_{chrom}–Fe^{III}_{cat}}$ has also been checked for various hydroxylation reactions (Table S5). Under the same conditions, the bimetallic complex exhibits similar TON (ca. 70) and A/K (ca. 12) values within this series, hence showing that the catalyst can be efficient and selective for a range of substrates.

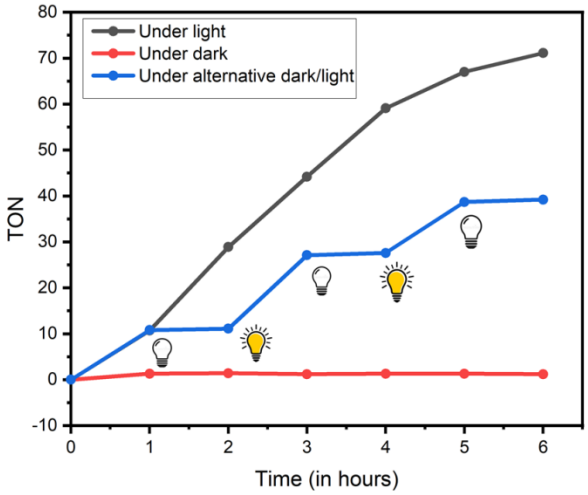

Figure 3. Time profile for photoinduced cyclohexane oxidation.

Time profile studies were carried out for cyclohexane oxidation using$\mathbf{Ru^{II}_{chrom}–Fe^{III}_{cat}}$(Figure 3). The reaction proceeds linearly with time upon illumination with a blue LED. Conversely, no catalytic conversion was observed upto 6 hours under dark conditions. A test reaction under the alternative environment of blue LED illumination and dark conditions has been monitored for a period of 6 hours.

Based on previous reports[57–59] and our results, two major mechanistic pathways may be proposed (Scheme 2). Pathway 1 is Fe-catalyst free pathway, in which the excited Ru(II)* may generate $^1O_2$as an active oxidant to carry out substrate oxidation.[58]This pathway does not play a significant role in C-H oxidation process. However, its presence cannot be ignored as they have shown their contribution in test reactions (Table 1: Entries 2-3).Pathway 2 involves the photoinduced e^- transfer between redox partners and reductive O_2 activation at Fe centre to generate iron-oxo species. This pathway is considered as the most probable route with the highest influence in catalytic conversion. During this event, upon light illumination into MLCT absorption band, Ru(II)* may easily transfer an electron to reduce covalently bound Fe(III) center. The resultant Fe(II) is sensitive to coordinate with O_2 to generate high valent Fe(IV)=O to subsequently carry out oxidation reactions. The oxidant Ru(III) is quenched to attain the ground state Ru(II) by the sacrificial e- donor.

Scheme 2. Plausible mechanistic pathways for photocatalytic oxidation reactions by $\mathbf{Ru^{II}_{chrom}–Fe^{III}_{cat}}$.

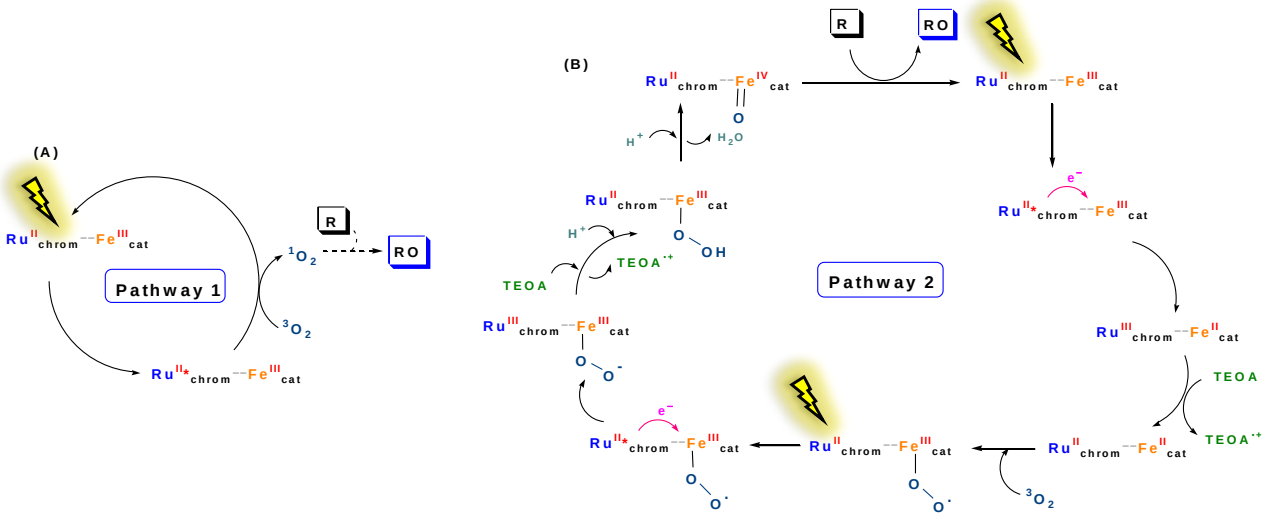

In conclusion, we demonstrate the first example of a non-heme based chromophore-catalyst system for reductive O_2 activation. Complex $\mathbf{Ru^{II}_{chrom}}$-$\mathbf{Fe^{III}_{cat}}$acts as an efficient photocatalyst for synthetically challenging C-H oxidation reactions. In comparison to a bimolecular $Ru(bpy)_3^{2+}$/$Fe(TPA)Cl_2$ catalytic system, the covalently bound dyad proved to be more efficient towards substrate oxidation. Therefore, it represents a promising alternative to the reported photoassisted Ru(II)-based systems.

Although the present study validates the concept, recent efforts are directed towards the optimization and deep mechanistic investigation of such systems. In particular, we are focused to improve the excited state properties of covalently bound chromophore/catalyst assemblies by modifying the ligands. The exploration and implementation of more potent oxidation catalysts are under process for their further use.

ASSOCIATED CONTENT

Supporting Information. Experimental details, XRD data (CCDC 2084261), NMR, ESI-MS, and electrochemical-data are provided in supporting information file.

AUTHOR INFORMATION

Corresponding Author

(Sushil Kumar)* *sushilvashisth@gmail.com*

ACKNOWLEDGMENT

SK acknowledges DST, New Delhi for financial assistance as Inspire Faculty Award (IFA-15-CH213).

REFERENCES

(1) Que, L.; Tolman, W. Biologically Inspired Oxidation Catalysis. *Nature***2008**, *455*, 333–40.

(2) Roduner, E.; Kaim, W.; Sarkar, B.; Urlacher, V. B.; Pleiss, J.; Gläser, R. Selective Catalytic Oxidation of C–H bonds with Molecular Oxygen. *ChemCatChem***2012**, *5*, 82–112.

(3) Costas, M.; Mehn, M. P.; Jensen, M. P.; Que, L. Jr. Oxygen Activation at Mononuclear Nonheme Iron: Enzymes, Intermediates and Models. *Chem. Rev.***2004**, *104*, 939−986.

(4) Ray, K.; Pfaff, F. F.; Wang, B.; Nam, W. Status of Reactive Nonheme Metal-Oxygen Intermediates in Chemical and Enzymatic Reactions. *J. Am. Chem. Soc.***2014**, *136*, 13942−13958.

(5) Rittle, J.; Green, M. T. Cytochrome P450 Compound I: Capture, Characterization, and C-H Bond Activation Kinetics. *Science***2010**, *330*, 933−937.

(6) Wallar, B. J.; Lipscomb, J. D. Dioxygen Activation by Enzymes Containing Binuclear Non-Heme Iron Clusters. *Chem. Rev.***1996**, *96*, 2625−2658.

(7) Tinberg, C. E.; Lippard, S. J. Dioxygen Activation in Soluble Methane Monooxygenase. *Acc. Chem. Res.***2011**, *44*, 280−288.

(8) Krebs, C.; Fujimori, D. G.; Walsh, C. T.; Bollinger, J. M., Jr. Non-Heme Fe(IV)−Oxo Intermediates. *Acc. Chem. Res.***2007**, *40*, 484−492.

(9) Proshlyakov, D. A.; Henshaw, T. F.; Monterosso, G. R.; Ryle, M. J.; Hausinger, R. P. Direct Detection of Oxygen Intermediates in the Non-Heme Fe Enzyme Taurine/α-Ketoglutarate Dioxygenase. *J. Am. Chem. Soc.***2004**, *126*, 1022−1023.

(10) Sinnecker, S.; Svensen, N.; Barr, E. W.; Ye, S.; Bollinger, J. M., Jr.; Neese, F.; Krebs, C. Spectroscopic and Computational Evaluation of the Structure of the High-Spin Fe(IV)-Oxo Intermediates in Taurine: α-Ketoglutarate Dioxygenase from Escherichia coli and Its His99Ala Ligand Variant. *J. Am. Chem. Soc.***2007**, *129*, 6168−6179.

(11) Kal, S.; Que, L., Jr. Dioxygen activation by nonheme iron enzymes with the 2-His-1-carboxylate facial triad that generate highvalent oxoiron oxidants. *JBIC, J. Biol. Inorg. Chem.***2017**, *22*, 339−365.

(12) O'Reilly, E.; Kohler, V.; Flitsch, S. L.; Turner, N. J. Cytochromes P450 as useful biocatalysts: addressing the limitations. *Chem. Commun.***2011**, *47*, 2490–2501.

(13) Rohde, J.-U.; In, J. H.; Lim, M. H.; Brennessel, W. W.; Bukowski, M. R.; Stubna, A.; Münck, E.; Nam, W.; Que, L., Jr. Crystallographic and Spectroscopic Evidence for a Nonheme FeIV=O Complex. *Science***2003**, *299*, 1037−1039.

(14) Nam, W. High-Valent Iron(IV)−Oxo Complexes of Heme and Non-Heme Ligands in Oxygenation Reactions. *Acc. Chem. Res.***2007**, *40*, 522−531.

(15) Que, L., Jr. The Road to Non-Heme Oxoferryls and Beyond. *Acc. Chem. Res.***2007**, *40*, 493−500.

(16) Hohenberger, J.; Ray, K.; Meyer, K. The Biology and Chemistry of High-Valent Iron−Oxo and Iron−Nitrido Complexes. *Nat. Commun.***2012**, *3*, 720−733.

(17) McDonald, A. R.; Que, L., Jr. High-Valent Nonheme Iron-Oxo Complexes: Synthesis, Structure, and Spectroscopy. *Coord. Chem. Rev.***2013**, *257*, 414−428.

(18) Tiago de Oliveira, F.; Chanda, A.; Banerjee, D.; Shan, X.; Mondal, S.; Que, L., Jr.; Bominaar, E. L.; Münck, E.; Collins, T. J. Chemical and spectroscopic evidence for an FeV-Oxo Complex. *Science***2007**, *315*, 835−838.

(19) Van Heuvelen, K. M.; Fiedler, A. T.; Shan, X.; De Hont, R. F.; Meier, K. K.; Bominaar, E. L.; Münck, E.; Que, L., Jr. One-electron oxidation of an oxoiron(IV) complex to form an [O=FeV=NR]+ center. *Proc. Natl. Acad. Sci. U. S. A.***2012**, *109*, 11933−11938.

(20) Serrano-Plana, J.; Oloo, W. N.; Acosta-Rueda, L.; Meier, K. K.; Verdejo, B.; García-España, E.; Basallote, M. G.; Münck, E.; Que, L., Jr.; Company, A.; Costas, M. Trapping a Highly Reactive Nonheme Iron Intermediate That Oxygenates Strong C-H Bonds with Stereoretention. *J. Am. Chem. Soc.***2015**, *137*, 15833−15842.

(21) Singh, R.; Ganguly, G.; Malinkin, S. O.; Demeshko, S.; Meyer, F.; Nordlander, E.; Paine, T. K. A Mononuclear Nonheme Iron(IV)-Oxo Complex of a Substituted N4Py Ligand: Effect of Ligand Field on Oxygen Atom Transfer and C–H Bond Cleavage Reactivity. *Inorg. Chem.***2019**, *58*,1862–1876.

(22) Bhattacharya, S.; Singh, R.; Paine, T. K. Effect of Ligand Fields on the Reactivity of O2 - Activating Iron(II)- Benzilate Complexes of Neutral N5 Donor Ligands. *Chem. Asian J.***2020**, *15*, 1360-1368

(23) Park, H.; Lee, D. Ligand Taxonomy for Bioinorganic Modeling of Dioxygen- Activating Non- Heme Iron Enzymes. *Chem. Eur. J.***2020**, *26*, 5916-5926.

(24) Oswald, V. F.; Lee, J. L.; Biswas, S.; Weitz, A. C.; Mittra, K.; Fan, R.; Li, J.; Zhao, J.; Hu, M. Y.; Alp, E. E.; Bominaar, E. L.; Guo, Y.; Green, M. T.; Hendrich, M. P.; Borovik, A. S. Effects of Noncovalent Interactions on High-Spin Fe(IV)–Oxido Complexes. *J. Am. Chem. Soc.***2020**, *142*, 11804-1181.

(25) Piquette, M. C.; Kryatov, S. V.; Rybak-Akimova, E. V. Kinetic Studies on the Oxoiron(IV) Complex with Tetradentate Aminopyridine Ligand PDP: Restoration of Catalytic Activity by Reduction with H2O2. *Inorg. Chem.***2019**, *58*, 13382-13393.

(26) Ehudin, M. A.; Quist, D. A.; Karlin, K. D. Enhanced Rates of C–H Bond Cleavage by a Hydrogen-Bonded Synthetic Heme High-Valent Iron(IV) Oxo Complex. *J. Am. Chem. Soc.***2019**, *141*, 12558-12569.

(27) Wang, L.; Gennari, M.; Reinhard, F. G. C.; Padamati, S. K.; Philouze, C.; Flot, D.; Demeshko, S.; Browne, W. R.; Meyer, F.; de Visser, S. P.; Duboc, C. O2 Activation by Non-Heme Thiolate-Based Dinuclear Fe Complexes, *Inorg. Chem.***2020**, *59*, 3249–3259

(28) Shimoyama, Y.; Kojima, T. Metal–Oxyl Species and Their Possible Roles in Chemical Oxidations. *Inorg. Chem.***2019**, *58*, 9517-9542.

(29) Ghosh, M.; Pattanayak, S.; Dhar, B. B.; Singh, K. K.; Panda, C.; Gupta, S. S. Selective C–H Bond Oxidation Catalyzed by the Fe-bTAML Complex: Mechanistic Implications. *Inorg. Chem.***2017**, *56*, 10852-10860.

(30) Collins, T. J.; Ryabov, A. D. Targeting of High-Valent Iron-TAML Activators at Hydrocarbons and Beyond. *Chem. Rev.***2017**, *117*, 9140-9162.

(31) Lindhorst, A. C.; Haslinger S.; Kühn, F. E. Molecular iron complexes as catalysts for selective C–H bond oxygenation reactions. Chem. Commun., **2015**, 51, 17193-17212.

(32) Herrero, C.; Nguyen-Thi, N.; Hammerer, F.; Banse, F.; Gagné, D.; Doucet, N.; Ricoux, R.; Mahy, J.-P.; Ricoux, R. Photoassisted Oxidation of Sulfides Catalyzed by Artificial Metalloenzymes using Water as an Oxygen Source. *Catalysts***2016**, *6*, 202.

(33) Fukuzumi, S.; Lee, Y.-M.; Nam W. Photocatalytic Oxygenation Reactions Using Water and Dioxygen, *ChemSusChem*, **2019**, *12*, 3931-3940.

(34) Mühldorf, B.; Lennert, U.; Wolf, R. Coupling Photoredox and Biomimetic Catalysis for the Visible-Light-Driven Oxygenation of Organic Compounds. In Chemical Photocatalysis, De Gruyter, **2020**, 223-244.

(35) Fukuzumi S.; Nam W. Thermal and Photoinduced Electron-Transfer Catalysis of High-Valent Metal-Oxo Porphyrins in Oxidation of Substrates. *J. Porphyrins Phthalocyanines***2016**, *20*, 1–10.

(36) Wilker, J. J.; Dmochowski, I. J.; Dawson, J. H.; Winkler, J. R.; Gray, H. B. Substrates for Rapid Delivery of Electrons and Holes to Buried Active Sites in Proteins. *Angew. Chem. Int. Ed.***1999**, *38*, 89-92.

(37) Ener, M. E.; Lee, Y.-T.; Winkler, J. R.; Gray, H. B.; Cheruzel, L. Photooxidation of cytochrome P450-BM3, *Proc. Natl. Acad. Sci.U.S.A.***2010**, *107*, 18783-18786.

(38) Tran, N.-H.; Huynh, N.; Bui, T.; Nguyen, Y.; Huynh, P.; Cooper, M. E.; Cheruzel, L. E. Light-Initiated Hydroxylation of Lauric Acid using Hybrid P450 BM3 Enzymes *Chem. Commun.***2011**, *47*, 11936-11938.

(39) Kotani, H.; Suenobu, T.; Lee, Y.-M.; Nam, W.; Fukuzumi, S. Photocatalytic Generation of a Non-Heme Oxoiron(IV) Complex with Water as an Oxygen Source *J. Am. Chem. Soc.***2011**, *33*, 3249-3251.

(40) Fukuzumi, S.; Kishi, T.; Kotani, H.; Lee, Y.-M.; Nam, W. Highly efficient photocatalytic oxygenation reactions using water as an oxygen source *Nat. Chem.***2011**, *3*, 38-41.

(41) Company, A.; Sabenya, G.; González-Béjar, M.; Gómez, L.; Clémancey, M.; Blondin, G.; Jasniewski, A. J.; Puri, M.; Browne, W. R.; Latour, J.-M.; Que, L., Jr.; Costas, M.; Pérez-Prieto, J.; Lloret-Fillol, J. Triggering the Generation of an Iron(IV)-Oxo Compound and Its Reactivity toward Sulfides by RuII Photocatalysis *J. Am. Chem. Soc.***2014**, *136*, 4624-4633.

(42) Chandra, B.; Singh, K. K.; Gupta, S. S. Selective Photocatalytic Hydroxylation and Epoxidation Reactions by an Iron Complex using Water as the Oxygen Source *Chem. Sci*. **2017**, *8*, 7545–7551.

(43) Herrero, C.; Quaranta, A.; Sircoglou, M.; Senechal-David, K.; Baron, A.; Marin, I. M.; Buron, C.; Baltaze, J.-P.; Leibl, W.; Aukauloo, A.; Banse, F. Successive Light Induced Two Electron Transfers in a Ru-Fe Supramolecular Assembly : from Ru-Fe(II)-OH2 to Ru-Fe(IV)-Oxo *Chem. Sci.***2015**, *6*, 2323- 2327.

(44) Avenier, F.; Herrero, C.; Leibl, W.; Desbois, A.; Guillot, R.; Mahy, J.-P.; Aukauloo, A. Photoassisted Generation of a Dinuclear Iron(III) Peroxo Species and Oxygen-Atom Transfer *Angew. Chem. Int. Ed.***2013**, *52*, 3634-3637.

(45) Chen, J.; Stepanovic, S.; Draksharapu, A.; Gruden M.; Browne, W. R. A Non-Heme Iron Photocatalyst for Light Driven Aerobic Oxidation of Methanol. *Angew. Chem. Int. Ed.***2018**, *57*, 3207-3211.

(46) Maliyackel, A. C.; Otvos, J. W.; Spreer, L. O.; Calvin, M. Photoinduced oxidation of a water-soluble manganese (III) porphyrin.*Proc. Natl. Acad. Sci. U.S.A.***1986**, *83*, 3572−3574.

(47) Bernd, M.; Wolf, R. C-H Photooxygenation of Alkyl Benzenes Catalyzed by Riboflavin Tetraacetate and a Non-Heme Iron Catalyst. *Angew. Chem. Int. Ed.* **2016**,*55*, 427−430.

(48) Vo, N. T.; Mekmouche, Y.; Tron, T.; Guillot, R.; Banse, F.; Halime, Z.; Sircoglou, M.; Leibl, W.; Aukauloo, A. A Reversible Electron Relay to Exclude Sacrificial Electron Donors in the Photocatalytic Oxygen Atom Transfer Reaction with O_2 in Water. *Angew. Chem. Int. Ed.***2019**, *58*, 16023−16027.

(49) (a) Mandon, D.; Machkour, A.; Goetz, S.; Welter, R.Trigonal Bipyramidal Geometry and Tridentate Coordination Mode of the Tripod in $FeCl_2$ Complexes with Tris(2-pyridylmethyl)amine Derivatives Bis-α-Substituted with Bulky Groups. Structures and Spectroscopic Comparative Studies. *Inorg. Chem.* **2002**, *41*, 5364-5372. (b) Mandon, D.; Jaafar, H.; Thibon, A. Exploring the Oxygen Sensitivity of $FeCl_2$ Complexes with Tris(2-pyridylmethyl)amine-Type Ligands: O_2 Coordination and a Quest for Superoxide. *New J. Chem.***2011**, *35*, 1986-2000.

(50) Arora, A.; Kaushal, J.; Kumar, A.; Kumar P.; Kumar, S. Ruthenium(II)-Polypyridyl-Based Sensor Bearing a DPA Unit for Selective Detection of Cu(II) Ion in Aqueous Medium. *ChemistrySelect*,**2019**, *4*, 6140-6147.

(51) Hua, S.-A.; Cattaneo, M.; Oelschlegel, M.; Heindl, M.; Schmid, L.; Dechert, S.; Wenger, O. S.; Siewert, I.; González, L.; Meyer, F. Electrochemical and Photophysical Properties of Ruthenium(II) Complexes Equipped with Sulfurated Bipyridine Ligands. *Inorg. Chem.***2020**, *59*, 4972–4984.

(52) Khade, R. V.; Choudhury, S. D.; Pal, H.; Kumbhar, A. S. Excited State Interaction of Ru(II) Imidazole Phenanthroline Complex $[Ru(bpy)_2ipH]^{2+}$ with 1,4-benzoquinone: Simple Electron Transfer or Proton Coupled Electron Transfer. **2018**, *19*, 2380-2388.

(53) Babini, E.; Bertini, I.; Borsari, M.; Capozzi, F.; Luchinat, C.; Zhang, X.; Moura, G. L. C.; Kurnikov, I. V.; Beratan, D. N.; Ponce, A.; Bilio, A. J. D.; Winkler, J. R.; Gray, H. B. Bond-Mediated Electron Tunneling in Ruthenium-Modified High-Potential Iron-Sulfur Protein, *J. Am. Chem. Soc.***2000**, *122*, 4532-4533.

(54) Kumar, S.; Singh, S.; Kumar, A.; Kumar P. Recognition, mechanistic investigation and applications for biorelevant $Cu^{2+}/Fe^{2+}/Fe^{3+}$ ions by ruthenium(II)-polypyridyl based fluorescent sensors" *Dalton Trans.***2021**, *50*, 2705-2721.

(55) Arias-Rotondo, D. M.; McCusker, J. K. The Photophysics of Photo Redox Catalysis: A Roadmap for Catalyst Design. *Chem. Soc. Rev*.**2016**, *45*, 5803-5820.

(56) Westhuizen, D. van der.; Eschwege, K. G. von.; Conradie, J. Electrochemistry and spectroscopy of substituted $[Ru(phen)_3]^{2+}$ and $[Ru(bpy)_3]^{2+}$ complexes. *Electrochim. Acta***2019**, *320*, 134540

(57) Iali, W.; Lanoe, P.-H.; Torelli, S.; Jouvenot, D.; Loiseau, F.; Lebrun, C.; Hamelin, O.; Menage, S. A. Ruthenium(II)–Copper(II) Dyad for the Photocatalytic Oxygenation of Organic Substrates Mediated by Dioxygen Activation. *Angew. Chem. Int. Ed.***2015**, *54*, 8415-8419.

(58) Bian, C.; Singh, A. K.; Niu, L.; Yi, H.; Lei, A. Visible-Light-Mediated Oxygenation Reactions using Molecular Oxygen. *Asian J. Org. Chem.***2017**, *6*, 386-396.

(59) Zhao, X.; Zhang, Y.; Wen, P.; Xu, G.; Ma, D.; Qiu, P. NH2-MIL-125 (Ti)/TiO_2 composites as superior visible-light photocatalysts for selective oxidation of cyclohexane. *Mol. Catal.***2018**, *452*, 175-183.

Graphical Abstract

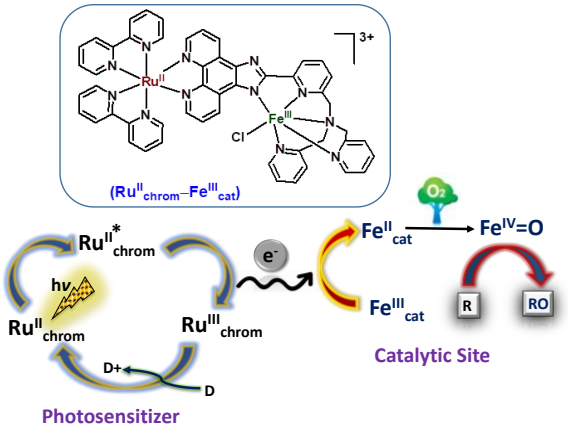

A novelheterobimetallic complex**Ru^{II}_{chrom}–Fe^{III}_{cat}**has been employed as photocatalyst for pertinent visible-light-driven C-H oxidation of different hydrocarbons in the presence of O_2 and a sacrificial agent.